Composites Science and Technology 151 (2017) 109–114

Contents lists available at ScienceDirect

Composites Science and Technology

journal homepage: http://www.elsevier.com/locate/compscitech

Nanocomposites with enhanced dielectric permittivity and breakdown strength by microstructure design of nanofillers

Ziming Cai [a], Xiaohui Wang [a, *], Bingcheng Luo [a], Wei Hong [b, c], Longwen Wu [a], Longtu Li [a, **]

[a] State Key Laboratory of New Ceramics and Fine Processing, School of Materials Science and Engineering, Tsinghua University, Beijing 100084, PR China
[b] Department of Aerospace Engineering, Iowa State University, Ames, IA 50010, USA
[c] Global Station for Soft Matter, Global Institution for Collaborative Research and Education, Hokkaido University, Sapporo, Japan

ARTICLE INFO

Article history:
Received 16 April 2017
Received in revised form
11 August 2017
Accepted 13 August 2017
Available online 15 August 2017

Keywords:
Nanocomposite
Dielectric permittivity
Breakdown strength
Orientation
Microstructure

ABSTRACT

Polymer-ceramic nanocomposites play an essential role in pulsed power system, due to their ultrahigh power density and fast charging–discharging capability. They also hold strong potential for improving the performance in energy storage capacitors, hybrid electric vehicles and kinetic energy weapons, since they contain a high-breakdown-strength polymer matrix and high-dielectric-permittivity ceramic nanofillers and thus can reach a high level of energy-storage density. In this work, through a finite element method and a phase field model, we theoretically analyze the nanocomposites with enhanced dielectric permittivity and dielectric breakdown strength by microstructure design of ceramic nanofillers, which covers the orientation, morphology and arrangement of nanofillers. Results indicate that the orientation of ceramic nanofibers has significant influence on the dielectric permittivity and breakdown strength of nanocomposites. The comparison of nanoparticles and nanofibers reveals the increase extent of interactions between polymer matrix and ceramic nanofillers can enhance the dielectric breakdown strength of the nanocomposites. Based on the results above, two sandwich structures consisting of both nanoparticles and nanofibers have been constructed to pursue a higher energy storage density.

1. Introduction

Dielectric materials possess fast charging-discharging capability and high power density, which are critical for the application in pulsed power system [1,2]. However, the low energy density limits their application in energy storage capacitors, hybrid electric vehicles and kinetic energy weapons [3–5]. In principle, the energy-storage density (J) of these devices can be written as

$$J = \int_0^{D_{max}} EdD \tag{1}$$

where E is electric field strength, D is dielectric displacement, and D_{max} is the dielectric displacement under saturated electric field strength. If we take dielectric permittivity ε as constant, the formula can be convert to

$$J = \frac{1}{2}\varepsilon {E_B}^2 \tag{2}$$

We can summarize that the dielectric permittivity (ε) and breakdown electric field (E_B) are two major factors that determine the energy storage density of dielectric materials. Polymer-ceramic nanocomposites show superior advantages to all other candidates, since that polymers are known for their high breakdown strength, meanwhile ceramic hold high dielectric permittivity [6–11]. Recent developments in polymer composites with nanosized ceramic fillers have reached high permittivity, high dielectric breakdown strength, low dielectric loss and long cycle life [12–21]. A maximum energy density of $> 30\ J/cm^3$ has been achieved in P(VDF-HFP)/BTO@TO_nfs nanocomposites [22]. The volume fraction, morphology, size, aspect ratio and orientation of ceramic nanofillers have been reported to have significant effect on the dielectric

* Corresponding author.
** Corresponding author.
E-mail addresses: wxh@mail.tsinghua.edu.cn (X. Wang), llt-dms@mail.tsinghua.edu.cn (L. Li).

http://dx.doi.org/10.1016/j.compscitech.2017.08.015
0266-3538/

permittivity and breakdown strength of nanocomposites [23–28], thus a property microstructure design of ceramic naonofillers is necessary for nanocomposites to obtain higher energy density.

In this work, we theoretically analyze the nanocomposite with enhanced dielectric permittivity and dielectric breakdown strength by microstructure design of ceramic nanofillers based on a finite element method and a phase field model, both implemented in COMSOL Multiphysics 5.2a. The structural design of the composite covers the orientation, morphology and arrangement of nanofillers [27–30]. The morphology of nanofillers used in our numerical model are nanofibers and nanoparticles, which are the most common nanofillers in previously reported works [31–34]. Firstly, four nanocomposites with different oriented nanofibers are simulated and compared. The effect of nanoparticles distribution in polymer matrix on the dielectric permittivity and breakdown strength on nanocomposites was studied in our previous work [35]. After that, the dielectric permittivity and breakdown strength of nanocomposites with preferred oriented nanofibers and with well distributed nanoparticles are separately calculated. It is found that under the same content of nanofillers, nanocomposite filled with well distributed nanoparticles (NNP) displays a higher dielectric permittivity, while nanocomposite filled with preferred oriented nanofibers (NNF) indicates a higher breakdown strength. Based on this conclusion and other related work [36–39], two sandwich-structured nanocomposite including both polymer/nanofibers layer and polymer/nanoparticles layer have been constructed to obtain both high dielectric permittivity and high breakdown strength, thus achieve high energy storage density.

2. Modeling process

2.1. Landau theory on ferroelectric ceramic nanofillers and phase field method on dielectric breakdown

The side length (L) of selected square region (R) of nanocomposites is set to 10 μm. As examples, two widely used filler and matrix materials, a ferroelectric ceramic barium titanate (BT) and a dielectric polymer poly(vinylidene fluoride) (PVDF) are adopted in our following calculations. The nanocomposites can be taken as a ferroelectric-dielectric system, for which the polymer matrix can be seen as linear dielectric, while the ceramic nanofillers are considered non-linear ferroelectric. The dielectric behavior of BT can be described through Landau's theory of phase transformation [40], which reads

$$\Delta G = \frac{1}{2}\alpha P^2 + \frac{1}{4}\beta P^4 + \frac{1}{6}\gamma P^6 - EP, \tag{3}$$

where P is the polarization, E is the applied electric field, and α, β and γ are the dielectric stiffness coefficients [40]. In stress-free polymer matrix, the equation of state of the electric field dependence of polarization and the dielectric response and its stability parallel to the applied electric field are given by Ref. [41].

$$\frac{\partial \Delta G}{\partial P} = 0 = \alpha P + \beta P^3 + \gamma P^5 - E, \tag{4}$$

$$\varepsilon_r(E) = \frac{1}{\varepsilon_0(\alpha + 3\beta P^2 + 5\gamma P^4)}, \tag{5}$$

$$\eta(E) = \frac{\varepsilon_r(E) - \varepsilon_r(E=0)}{\varepsilon_r(E=0)}. \tag{6}$$

The dielectric response of nanocomposites is simulated using COMSOL Multiphysics. The effective dielectric permittivity can be calculated from Ref. [42].

$$\varepsilon_r = \mathrm{d}\frac{\int D\cdot E\mathrm{d}V}{\varepsilon_0 A U^2}. \tag{7}$$

The study of the dielectric breakdown process of nanocomposites follows closely the phase field model developed in Refs. [43,44], by drawing an analogy between dielectric breakdown and mechanical fracture. A huge advantage of this method is that it can visualize the breakdown pathways and calculate the normalized breakdown strength. Instead of tracking individual breakdown pathways, a continuous scalar phase field s (x, t) is introduced to characterize the evolution process of a dielectric medium which turns into conductive at full damage. The value of s varies from 1 to 0, which respectively represent the intact state and the fully damaged state. The fully damaged material becomes conductive. Numerically, a large but finite permittivity ε_0/η is taken for such material part, where ε_0 is the initial permittivity and η is a small enough number. For any other intermediate state of nanocomposites, the permittivity is interpolated by

$$\varepsilon(s) = \frac{\varepsilon_0}{f(s) + \eta}, \tag{8}$$

where $f(s) = 4s^3 - 3s^4$. Breakdown happens if the process decreases the total potential energy of the system

$$\Pi[s,\phi] = \int_{\Omega} [W_{es}(E,s) + W_d(s) + W_i(\nabla s)]\mathrm{d}V, \tag{9}$$

where $W_{es}(E,s) = -\frac{\varepsilon}{2}E\cdot E$ is the complementary electrostatic energy per unit volume, $W_d(s) = W_c[1 - f(s)]$ is the breakdown energy function with W_c representing the critical density of electrostatic energy, $W_i(\nabla s) = \frac{\Gamma}{4}\nabla s\cdot\nabla s$ is the gradient energy term to regulate sharp phase boundaries. It is worth noting that the material parameter Γ is approximately the breakdown energy [41]. According to linear kinetic law: $\partial s/\partial t = -m\delta\Pi/\delta s$, the evolution equation for breakdown variable s can be achieved after substituting in detailed forms of the energy functions:

$$\frac{1}{m}\frac{\partial s}{\partial t} = \frac{\varepsilon'(s)}{2}\nabla\phi\cdot\nabla\phi + W_c f'(s) + \frac{\Gamma}{2}\nabla^2 s. \tag{10}$$

Here, mobility m is a material parameter that features the speed of breakdown propagation in nanocomposites. To facilitate numerical simulation, we will normalize energies by Γ, time by mΓ, and electric potentials by $\sqrt{\Gamma/\varepsilon_0}$. The normalized governing equations of dimensionless form can be written as:

$$\overline{\nabla}\cdot\left[\frac{1}{f(s) + \eta}\overline{\nabla\phi}\right] = 0, \tag{11}$$

$$\frac{\partial s}{\partial \bar{t}} = -\frac{f'(s)}{2[f(s)+\eta]^2}\overline{\nabla\phi}\cdot\overline{\nabla\phi} + f'(s) + \frac{1}{2}\overline{\nabla}^2 s, \tag{12}$$

in which the corresponding quantities are symbolized with overbars. While the above described model considers only linear dielectrics, here in this study we add the nonlinear performance of nanoceramic by normalizing Eqs. (4) and (5) into:

$$\alpha\overline{P} + \beta\overline{P}^3 + \gamma\overline{P}^5 - \overline{E} = 0, \tag{13}$$

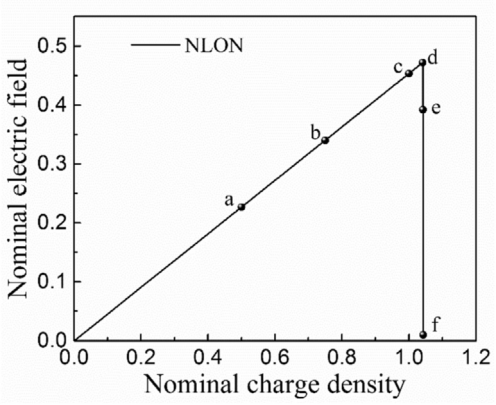

Fig. 1. The nominal field-charge-density relation of nanocomposite with laterally oriented nanofibers (NLON). The point a to f are corresponding to the Fig. 2 (a) to (f).

$$\varepsilon_r(\overline{E}) = \frac{1}{\varepsilon_0\left(\alpha + 3\beta\overline{P}^2 + 5\gamma\overline{P}^4\right)}. \tag{14}$$

With the focus mainly on the mechanism study of dielectric response and breakdown process, all simulations are carried out in two-dimensional (2D) domains. The detailed simulation information can be found in our recent work [35].

3. Results and discussion

3.1. Dielectric permittivity and breakdown behavior of nanocomposites with different oriented nanofibers

Four nanocomposites with different oriented nanofibers has been generated through MATLAB and COMSOL and the content of nanofibers is all set as 10% as seen in the insets in Fig. 3 or Fig. 4. The

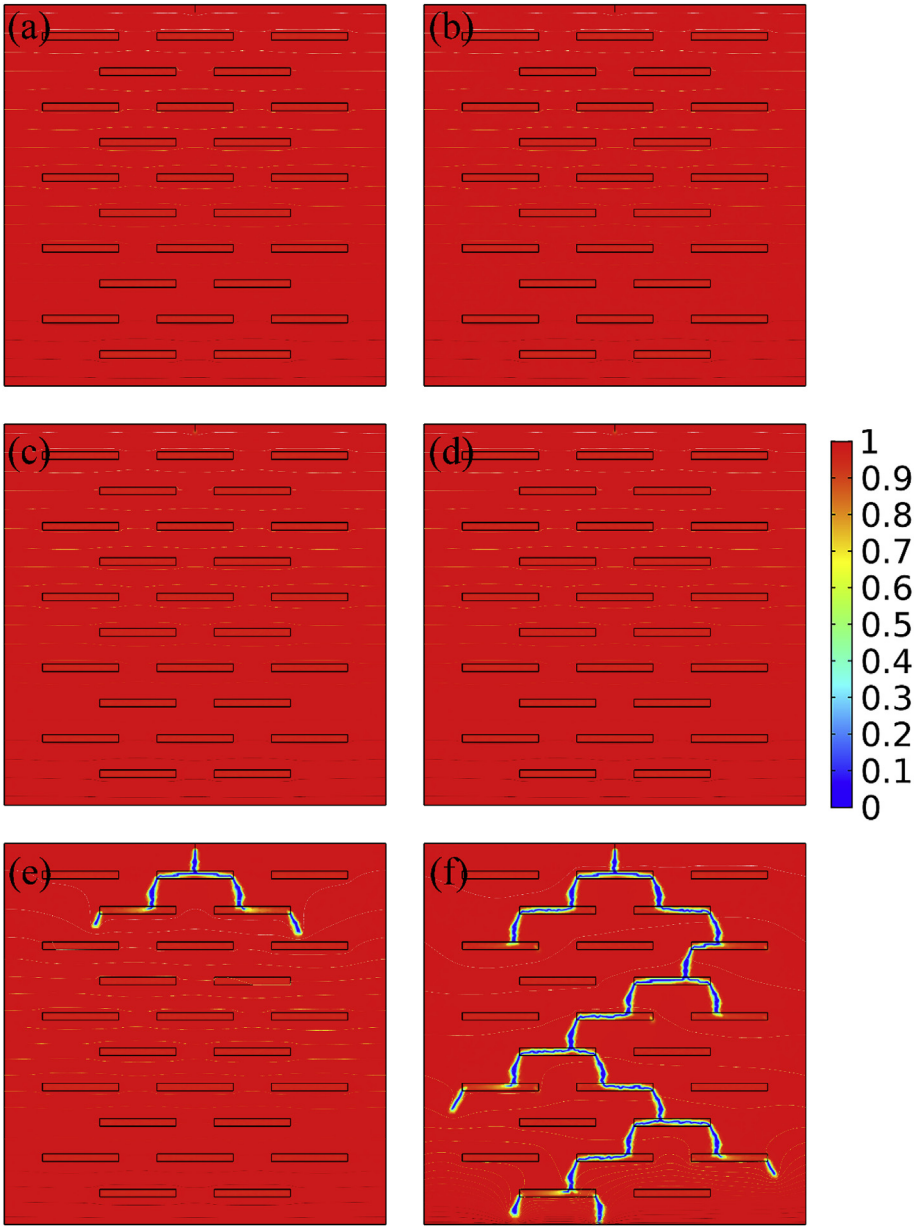

Fig. 2. (a) to (f) Snapshots of the breakdown process of nanocomposite of nanocomposite with laterally oriented nanofibers (NLON), indicating the evolution of the breakdown channel. (a) to (f) correspond to the six dots a to f on Fig. 1.

nanofiber length is set as 2 μm and the diameter is 0.2 μm. The orientations of nanofibers are along the applied electric field, in the lateral direction, or randomly distributed (two cases). The breakdown path pattern at different field strength of nanocomposite with laterally oriented nanofibers (NLON) is given in Fig. 1. Fig. 2. (a) to (f) are snapshots of the breakdown process of NLON, indicating the evolution of the breakdown channel. (a) to (f) correspond to the six dots a to f on Fig. 1. It is a very valid proof that those breakdown branches only appear at close to breakdown field strength. When the applied electric field reaches a certain value, the breakdown channel is formed instantly. Therefore, the assumption of linear response in energy density calculation is reasonable in these cases.

The results are marked as parallel, perpendicular, random 1 and random 2, respectively, as shown in Fig. 3 and Fig. 4. It can be tell from Fig. 3 that the orientation of nanofibers has tremendous impact on the dielectric permittivity of nanocomposites. The dielectric permittivity of nanocomposite with parallelly oriented nanofibers (NPON) is almost twice larger than nanocomposite with laterally oriented nanofibers (NLON) at low electric field, while the dielectric permittivity of nanocomposite with randomly oriented nanofibers (NRON) is between them. Along with the increase of applied electric field, the dielectric permittivity of NPON and NRON drops sharply due to the dielectric nonlinearity of the ceramic nanofillers, while the dielectric permittivity of NLON shows a high stability. Such huge difference in permittivity is resulted from the difference of the distribution of local electric field as seen in the insets in Fig. 3. When the orientation of nanofibers is in parallel with the applied electric field, the local electric field will concentrate a lot at the upper and lower ends, which leads to a larger electric displacement at the same time. It will in turn enhance the total energy density of the nanocomposites, thus make the nanocomposites showing a higher dielectric permittivity. The more the proportion of parallel oriented nanofibers, the larger the dielectric permittivity. The nanofibers share little electric field compared with the polymer matrix, due to the enormous difference between ceramic nanofibers and polymer matrix in dielectric permittivity. That is the reason the dielectric permittivity of nanocomposites can hold stable at the beginning of applied electric field increase. However, along the applied electric field increases, the local electric field concentrated more at the upper and lower ends, the electric field inside the nanofibers gradually rises. The dielectric permittivity of nanofibers starts to reduce because of its intrinsic nonlinear effect, which results in the decrease in dielectric permittivity of nanocomposites at a certain applied electric field. Yet, the NLON is narrow along the direction of applied electric field, the electric field inside the nanofibers change slightly, which makes it quite stable in dielectric permittivity.

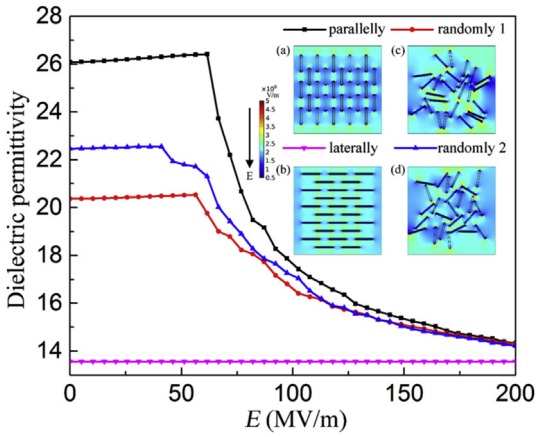

Fig. 3. The effective dielectric response of nanocomposites with different oriented nanofibers at various applied electric field (E). The insets are the electric field distribution of nanocomposites: (a) with parallel oriented nanofibers (marked as parallel), (b) with vertical oriented nanofibers (marked as vertical), (c) with random oriented nanofibers (marked as random 1), (d) with random oriented nanofibers (marked as random 2), against applied electric field at 200 MV/m.

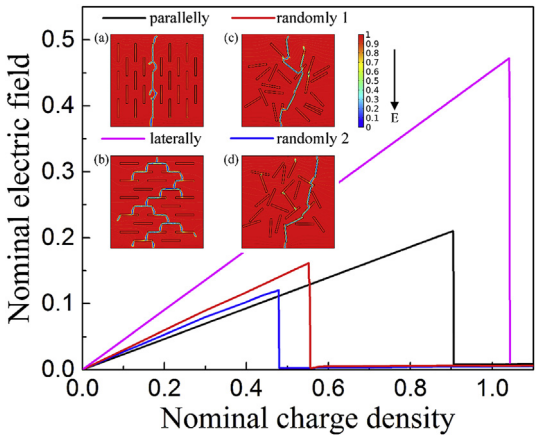

Fig. 4. The nominal field-charge-density relation of nanocomposites with different oriented nanofibers. The insets are dielectric breakdown paths of nanocomposites: (a) with parallel oriented nanofibers (marked as parallel), (b) with vertical oriented nanofibers (marked as vertical), (c) with random oriented nanofibers (marked as random 1), (d) with random oriented nanofibers (marked as random 2).

The distribution of electric field analyzed above has a close relationship with the dielectric breakdown of these nanocomposites. The following results of phase field modeling reveal the details of dielectric breakdown in nanocomposites. The nominal field-charge-density relation of nanocomposites with different oriented nanofibers is presented in Fig. 4, where the maximum value of nominal electric field is taken as the nominal breakdown strength of the nanocomposites and the insets are the breakdown paths of different nanocomposites. We can easily figure out that the NLON shows the highest breakdown strength, and it is almost 2.5 times larger than NPON and 3 times larger than NRON. The reason why there is a such big difference in breakdown strength of nanocomposites is that the orientation of nanofibers has a significant influence on the distribution of local electric field in nanocomposites as seen in the insets in Fig. 3. In the meanwhile, the breakdown strength of nanofibers is weaker than the polymer matrix, so the breakdown path will eventually pass through the ceramic nanofibers. The breakdown will begin at certain place where the electric field is the most concentrated, and then the nanofibers which are approximately parallelly oriented and near the initial breakdown area will be the fast channel of the entire breakdown as seen in the insets in Fig. 4. The NLON cannot provide such fast channel along the direction of applied electric field and it can extend the breakdown path in the vertical direction of applied electric field, which both result in its high breakdown strength. The dielectric breakdown strength of two NRON cases is even lower than that of NPON, since there is great opportunity for ceramic nanofibers to get connected with each other in polymer matrix. Therefore, it is easier to form a breakdown channel inside the weaker ceramic nanofibers. The initial slope of the field-charge-density curve is inversely proportional to the permittivity of nanocomposites, and it performs consistently with the results in Fig. 3. Base on the above, we can find that the NLON is a good candidate for the application in energy storage, especially working in high electric field.

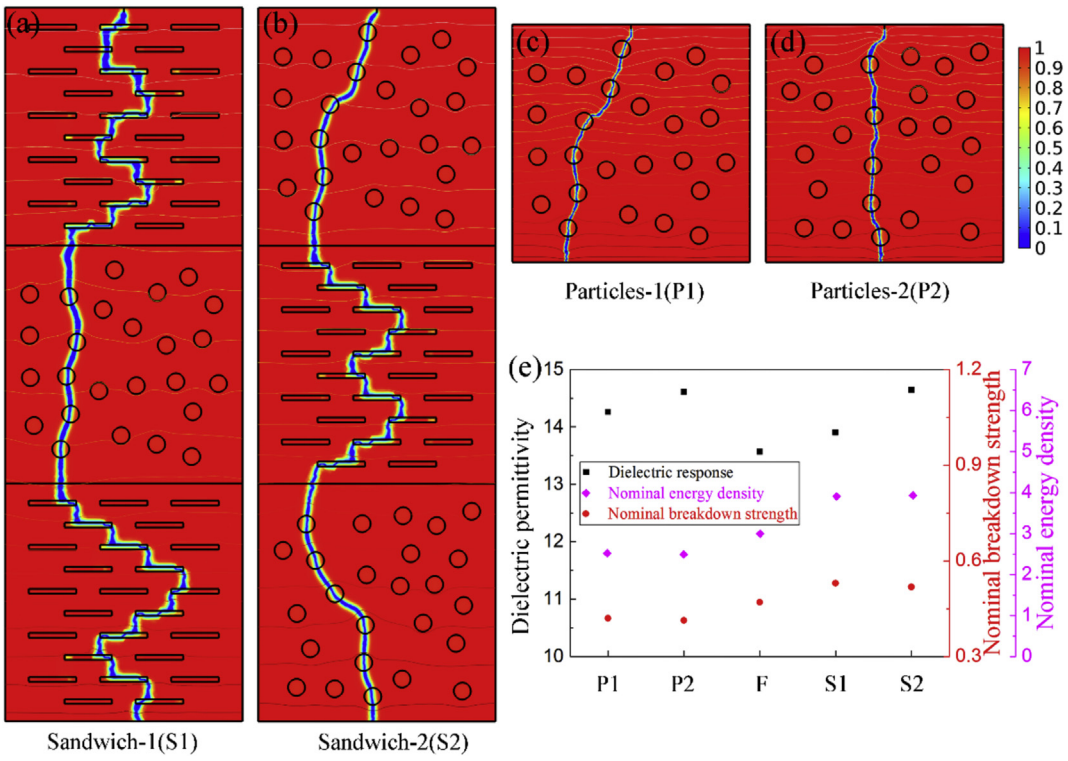

Fig. 5. The breakdown paths of nanocomposites with (a) Sandwich-1 (S1), (b) Sandwich-2 (S2), (c) Particles-1 (P1), (d) Particles-2 (P2) microstructures. (e) Dielectric permittivity, nominal breakdown strength and nominal energy density of nanocomposites with different microstructures of nanofillers at the same content of 10%.

3.2. Dielectric permittivity and breakdown behavior of nanocomposites with designed microstructure of nanofibers

In contrast, the nanocomposites with same content (10%) nanoparticles are simulated as shown in Fig. 5(c), (d) and respectively marked as Particles-1 (P1), Particles-2 (P2). The nanoparticles distribution of these two cases is controlled fairly well according to our previous work [35]. It is found that under the same content of nanofillers, nanocomposite filled with well-distributed nanoparticles (NNP) displays a higher dielectric permittivity, while nanocomposite filled with preferentially oriented nanofibers (NNF) exhibits a higher breakdown strength, which can be obtained in Fig. 5(e). Based on this results and other related work, two sandwich-structured nanocomposite including both polymer/nanofibers layer and polymer/nanoparticles layer have been constructed.

Sandwich-1 (S1) contains NNP in the top and bottom layers and NNF in the middle layer, while Sandwich-2 (S2) contains NNF in the top and bottom layers and NNP in the middle layer, as shown in Fig. 5(a) and (b). The volume fraction of nanofillers is kept at 10%. The nominal energy density can be calculated using equation (2) if taking the nanocomposites as approximately linear dielectric. At last, the breakdown paths of NNP and sandwich structures are shown in Fig. 5(a)–(d) and the dielectric permittivity, nominal breakdown strength and nominal energy density of nanocomposites with different microstructures of nanofillers are seen in Fig. 5(e). It is obviously that the nanocomposites with sandwich microstructure combine the advantage of the high permittivity NNP and the high breakdown strength NNF. The nominal breakdown strength is even high than any nanocomposites with nanofibers or nanoparticles due to this special designed sandwich structure. Thus the nominal energy density of such nanocomposites is enhanced a lot as seen in Fig. 5(e). It is worth noting that the trend of nominal energy density is closer to the nominal breakdown strength, which means the breakdown strength is quite an important property that determine the energy density of nanocomposite. It can also be summarized from equation (2), where energy density is proportional to the square of breakdown strength.

4. Conclusion

In summary, a phase-field model is developed to simulate the dielectric permittivity and breakdown behavior of polymer-ceramic nanocomposites, and solved numerically with the finite element method. The microstructural design of the composites, including the orientation, morphology and arrangement of nanofillers, has a dramatic influence on the dielectric properties of nanocomposites. The dielectric permittivity of NPON is almost twice larger than NLON. However, when it comes to breakdown strength, NLON is almost 2.5 times larger than NPON. The two effects combined, NLON is a better candidate for energy storage. It is found that under the same volume fraction of nanofillers, NNP displays a higher dielectric permittivity, while NNF shows a higher breakdown strength. Inspired by these results, two sandwich-structured nanocomposites including both polymer/nanofibers layer and polymer/nanoparticles layer have been constructed. Results indicate that such structures combine the advantages of both the high permittivity NNP and the high breakdown strength NNF, thus achieving high energy storage density and are perfect candidates for energy-storage applications.

Acknowledgments

The work was supported by Ministry of Sciences and Technology of China through National Basic Research Program of China (973 Program 2015CB654604), National Natural Science Foundation of China (Grant No. 51272123, 51672148), and also supported by CBMI

Construction Co., Ltd. In addition, our work is completed on the "Explorer 100" cluster system of Tsinghua National Laboratory for Information Science and Technology.

References

[1] Z.-M. Dang, J.-K. Yuan, S.-H. Yao, R.-J. Liao, Flexible nanodielectric materials with high permittivity for power energy storage, Adv. Mater 25 (2013) 6334–6365.

[2] Q. Li, K. Han, M.R. Gadinski, G. Zhang, Q. Wang, High energy and power density capacitors from solution-processed ternary ferroelectric polymer nanocomposites, Adv. Mater 26 (2014) 6244–6249.

[3] B.C. Riggs, S. Adireddy, C.H. Rehm, V.S. Puli, R. Elupula, D.B. Chrisey, Polymer nanocomposites for energy storage applications, Mater. Today Proc. 2 (2015) 3853–3863.

[4] C. Yang, H. Wei, L. Guan, J. Guo, Y. Wang, X. Yan, X. Zhang, S. Wei, Z. Guo, Polymer nanocomposites for energy storage, energy saving, and anticorrosion, J. Mater. Chem. A 3 (2015) 14929–14941.

[5] N.C. Goulbourne, A. Barhoumi Meddeb, Z. Ounaies, Z. Ounaies, Nano-enhanced Polym. Compos. energy storage Appl. 8342 (2012) 834207.

[6] Y. Hao, X. Wang, K. Bi, J. Zhang, Y. Huang, L. Wu, P. Zhao, K. Xu, M. Lei, L. Li, Significantly enhanced energy storage performance promoted by ultimate sized ferroelectric $BaTiO_3$ fillers in nanocomposite films, Nano Energy 31 (2017) 49–56.

[7] G. Landi, A. Sorrentino, F. Fedi, H.C. Neitzert, S. Iannace, Cycle stability and dielectric properties of a new biodegradable energy storage material, Nano Energy 17 (2015) 348–355.

[8] Q. Chen, Y. Shen, S. Zhang, Q.M. Zhang, Polymer-based dielectrics with high energy storage density, Annu. Rev. Mater. Res. 45 (2015) 433–458.

[9] X. Hao, A review on the dielectric materials for high energy-storage application, J. Adv. Dielectr. 03 (2013) 1330001.

[10] Q. Wang, L. Zhu, Polymer nanocomposites for electrical energy storage, J. Polym. Sci. Part B Polym. Phys. 49 (2011) 1421–1429.

[11] Q. Zhang, F. Gao, C. Zhang, L. Wang, M. Wang, M. Qin, G. Hu, J. Kong, Enhanced dielectric tunability of $Ba_{0.6}Sr_{0.4}TiO_3$/Poly (vinylidene fluoride) composites via interface modification by silane coupling agent, Compos. Sci. Technol. 129 (2016) 93–100.

[12] S. Liu, S. Xiu, B. Shen, J. Zhai, L. Kong, Dielectric properties and energy storage densities of poly(vinylidenefluoride) nanocomposite with surface hydroxylated cube shaped $Ba_{0.6}Sr_{0.4}TiO_3$ nanoparticles, Polymers 8 (2016) 45.

[13] S. Liu, S. Xiao, S. Xiu, B. Shen, J. Zhai, Z. An, Poly (vinylidene fluoride) nanocomposites capacitors with significantly enhanced dielectric constant and energy density by filling with surface-fluorinated $Ba_{0.6}Sr_{0.4}TiO_3$ nanofibers, Rsc Adv. 5 (2015) 40692–40699.

[14] S. Liu, J. Zhai, J. Wang, S. Xue, W. Zhang, Enhanced energy storage density in poly(vinylidene fluoride) nanocomposites by a small loading of suface-hydroxylated Ba0.6Sr0.4TiO3 nanofibers, ACS Appl. Mater. Interfaces 6 (2014) 1533–1540.

[15] H. Tang, H.A. Sodano, Ultra high energy density nanocomposite capacitors with fast discharge using $Ba_{0.2}Sr_{0.8}TiO_3$ nanowires, Nano Lett. 13 (2013) 1373–1379.

[16] P. Hu, Y. Song, H. Liu, Y. Shen, Y. Lin, C.-W. Nan, Largely enhanced energy density in flexible P(VDF-TrFE) nanocomposites by surface-modified electrospun $BaSrTiO_3$fibers, J. Mater. Chem. A 1 (2013) 1688–1693.

[17] S. Rajesh, K. Sonoda, A. Uusimaki, K.H. Yang, H.Y. Lu, H. Jantunen, Effective dielectric response of polymer composites with ceramic coated silver flakes, J. Mater. Sci. Mater. Electron. 24 (2012) 191–195.

[18] L. Xie, X. Huang, C. Wu, P. Jiang, Core-shell structured poly(methyl methacrylate)/$BaTiO_3$ nanocomposites prepared by in situ atom transfer radical polymerization: a route to high dielectric constant materials with the inherent low loss of the base polymer, J. Mater. Chem. 21 (2011) 5897–5906.

[19] P. Kim, N.M. Doss, J.P. Tillotson, P.J. Hotchkiss, M.J. Pan, S.R. Marder, J. Li, J.P. Calame, J.W. Perry, High energy density nanocomposites based on surface-modified $BaTiO_3$ and a ferroelectric polymer, Acs Nano 3 (2009) 2581–2592.

[20] K. Wu, C. Lei, W. Yang, S. Chai, F. Chen, Q. Fu, Surface modification of boron nitride by reduced graphene oxide for preparation of dielectric material with enhanced dielectric constant and well-suppressed dielectric loss, Compos. Sci. Technol. 134 (2016) 191–200.

[21] M. Donnay, S. Tzavalas, E. Logakis, Boron nitride filled epoxy with improved thermal conductivity and dielectric breakdown strength, Compos. Sci. Technol. 110 (2015) 152–158.

[22] X. Zhang, Y. Shen, B. Xu, Q. Zhang, L. Gu, J. Jiang, J. Ma, Y. Lin, C.W. Nan, Giant energy density and improved discharge efficiency of solution-processed polymer nanocomposites for dielectric energy storage, Adv. Mater. 28 (2016) 2055–2061.

[23] S.P. Fillery, H. Koerner, L. Drummy, E. Dunkerley, M.F. Durstock, D.F. Schmidt, R.A. Vaia, Nanolaminates: increasing dielectric breakdown strength of composites, ACS Appl. Mater. Interfaces 4 (2012) 1388–1396.

[24] N. Guo, S.A. DiBenedetto, P. Tewari, M.T. Lanagan, M.A. Ratner, T.J. Marks, Nanoparticle, size, shape, and interfacial effects on leakage current density, permittivity, and breakdown strength of metal oxide-polyolefin nanocomposites: experiment and theory, Chem. Mater 22 (2010) 1567–1578.

[25] D. Tan, Y. Cao, E. Tuncer, P. Irwin, Nanofiller dispersion in polymer dielectrics, Mater. Sci. Appl. 04 (2013) 6–15.

[26] B. Luo, X. Wang, Y. Wang, L. Li, Fabrication, characterization, properties and theoretical analysis of ceramic/PVDF composite flexible films with high dielectric constant and low dielectric loss, J. Mater. Chem. A 2 (2014) 510–519.

[27] Y.U. Wang, D.Q. Tan, Computational study of filler microstructure and effective property relations in dielectric composites, J. Appl. Phys. 109 (2011) 104102.

[28] Y.U. Wang, Phase field model of dielectric and magnetic composites, Appl. Phys. Lett. 96 (2010) 232901.

[29] V. Tomer, G. Polizos, C.A. Randall, E. Manias, Polyethylene nanocomposite dielectrics: implications of nanofiller orientation on high field properties and energy storage, J. Appl. Phys. 109 (2011) 074113.

[30] V. Tomer, E. Manias, C.A. Randall, High field properties and energy storage in nanocomposite dielectrics of poly(vinylidene fluoride-hexafluoropropylene), J. Appl. Phys. 110 (2011) 044107.

[31] X. Zhang, Y. Shen, Q. Zhang, L. Gu, Y. Hu, J. Du, Y. Lin, C.W. Nan, Ultrahigh energy density of polymer nanocomposites containing $BaTiO_3$@TiO_2 nanofibers by atomic-scale interface engineering, Adv. Mater 27 (2015) 819–824.

[32] S. Luo, S. Yu, R. Sun, C.P. Wong, Nano Ag-deposited $BaTiO_3$ hybrid particles as fillers for polymeric dielectric composites: toward high dielectric constant and suppressed loss, ACS Appl. Mater. Interfaces 6 (2014) 176–182.

[33] Z. Wang, J.K. Nelson, H. Hillborg, S. Zhao, L.S. Schadler, Dielectric constant and breakdown strength of polymer composites with high aspect ratio fillers studied by finite element models, Compos. Sci. Technol. 76 (2013) 29–36.

[34] Y. Song, Y. Shen, H. Liu, Y. Lin, M. Li, C.-W. Nan, Improving the dielectric constants and breakdown strength of polymer composites: effects of the shape of the BaTiO3 nanoinclusions, surface modification and polymer matrix, J. Mater. Chem. 22 (2012) 16491–16498.

[35] Z. Cai, X. Wang, B. Luo, W. Hong, L. Wu, L. Li, Dielectric response and breakdown behavior of polymer-ceramic nanocomposites: the effect of nanoparticle distribution, Compos. Sci. Technol. 145 (2017) 105–113.

[36] Q. Li, F. Liu, T. Yang, M.R. Gadinski, G. Zhang, L.Q. Chen, Q. Wang, Sandwich-structured polymer nanocomposites with high energy density and great charge-discharge efficiency at elevated temperatures, Proc. Natl. Acad. Sci. U. S. A. 113 (2016).

[37] C. Jiang, D. Zhang, K. Zhou, X. Zhou, H. Luo, I. Abrahams, Significantly enhanced energy storage density of sandwich-structured $(Na_{0.5}Bi_{0.5})_{0.93}Ba_{0.07}TiO_3$/P(VDF-HFP) composites induced by PVP-modified two-dimensional platelets, J. Mater. Chem. A 4 (2016) 18050–18059.

[38] Y. Shen, Y. Hu, W. Chen, J. Wang, Y. Guan, J. Du, X. Zhang, J. Ma, M. Li, Y. Lin, Modulation of topological structure induces ultrahigh energy density of graphene/$Ba_{0.6}Sr_{0.4}TiO_3$ nanofiber/polymer nanocomposites, Nano Energy 18 (2015) 176–186.

[39] P. Hu, Y. Shen, Y. Guan, X. Zhang, Y. Lin, Q. Zhang, C.-W. Nan, Topological-Structure modulated polymer nanocomposites exhibiting highly enhanced dielectric strength and energy density, Adv. Funct. Mater 24 (2014) 3172–3178.

[40] Y.L. Wang, A.K. Tagantsev, D. Damjanovic, N. Setter, V.K. Yarmarkin, A.I. Sokolov, I.A. Lukyanchuk, Landau thermodynamic potential for $BaTiO_3$, J. Appl. Phys. 101 (2007), 104115–104115-104119.

[41] K. Zhou, S.A. Boggs, R. Ramprasad, M. Aindow, C. Erkey, S.P. Alpay, Dielectric response and tunability of a dielectric-paraelectric composite, Appl. Phys. Lett. 93 (2008) 3.

[42] K. Zhou, S. Boggs, 2009 IEEE Pulsed Power Conference, IEEE, 2009, pp. 342–345.

[43] W. Hong, K.C. Pitike, Modeling breakdown-resistant composite dielectrics, in: K. Volokh, M. Jabareen (Eds.), Iutam Symposium on Mechanics of Soft Active Materials, Elsevier Science Bv, Amsterdam, 2015, pp. 73–82.

[44] K.C. Pitike, W. Hong, Phase-field model for dielectric breakdown in solids, J. Appl. Phys. 115 (2014) 8.